Materials Transactions, Vol. 53, No. 1 (2012) pp. 185 to 190

Determination of the Load Carrying Capacity of Damaged Pipes Using Local Approach to Fracture

Bojan Medjo[1,*], Marko Rakin[1], Miodrag Arsić[2], Živče Šarkoćević[3], Milorad Zrilić[1] and Slaviša Putić[1]

[1]*Faculty of Technology and Metallurgy, Karnegijeva 4, Belgrade, Serbia*
[2]*Institute for Testing of Materials (IMS), Bulevar vojvode Mišića 43, Belgrade, Serbia*
[3]*High Technical School of Professional Studies, Nušićeva 6, Zvečan, Serbia*

The subject of this study was the application of local approach to ductile fracture in order to estimate the integrity of damaged seam casing pipes for oil and gas drilling rigs. The experimental testing included tensile testing of specimens and a pressure test of a pipe with different levels of damage simulated by machined notches. In exploitation, such structures (i.e., pipes with local thin areas) can fail by the ductile fracture mechanism or by plastic collapse in the ligament. However, the majority of the procedures for determining their integrity are based on limit loads, i.e., plastic collapse criteria. In this work, a pipe subjected to internal pressure was modelled using the finite element method and local approach to fracture (the Complete Gurson Model - CGM), with the aim of determining damage development in the material (i.e., at the bottom of a machined defect) and of establishing the criteria for the maximum pressure that a damaged pipe can withstand. The results obtained using the micromechanical model are discussed and compared with several often used limit load expressions from the literature and a stress-based finite element criterion. It is shown that local approach can give appropriate results and represent failure criterion for pipes with local thin areas.
[doi:10.2320/matertrans.M2011210]

(Received July 11, 2011; Accepted October 21, 2011; Published December 14, 2011)

Keywords: *casing pipe, simulated corrosion defect, local approach, finite element method, maximum pressure*

1. Introduction

Pipelines consisting of seam or seamless pipes are the most economic and safest way for oil and gas exploitation and transport. Decreases in strength caused by corrosion defects are very often encountered in these structures; they can endanger work safety and even lead to catastrophic failures. Therefore, pipelines should be controlled in certain time intervals, in order to obtain a realistic insight into the possible propagation of damage and assess their structural integrity. Many procedures for estimating the remaining strength of pipes with corroded areas have hitherto been developed.[1–8)]

One of the solutions for an assessment of the influence of corrosion defects on pipe integrity is the ASME B31G code, published in Ref. 1). Since it is often regarded as too conservative, several other procedures have been derived from it, such as the modification by Kiefner and Vieth[2)] (in the remainder of the text - modified ASME B31G) and RSTRENG.[3)] Det Norske Veritas (DNV) published recommended practices[4)] for assessing the integrity of corroded pipelines under internal pressure and internal pressure combined with axial loading. FITNET procedures[5)] also contain a module for estimating the remaining strength of pipelines with local corrosion damage.

Choi *et al.*[6)] derived limit load solutions based on the results of experimental and numerical analyses. A series of burst tests were conducted and corresponding elastic–plastic finite element simulations were performed. Failure was predicted to occur when the von Mises stress reached a reference stress across the entire ligament; the reference stress was determined as 80–90% of the ultimate tensile stress. This value depends on the geometry of the defect, and two different shapes were studied: elliptical and rectangular. Adib-Ramezani *et al.*[7)] proposed integrity assessment of the pipes with defects under internal pressure based on a modification of the SINTAP (Structural Integrity Assessment Procedure).[9)] The FAD concept for integrity assessment of cracked structures was extended to notch problems; in this way, the assessment accounted for both collapse limit loads and the fracture aspect.

As mentioned previously, failure of pipelines with local thin areas (e.g., corrosion defects) can be caused either by plastic collapse or fracture.[10–13)] However, in the literature, the critical loading for such structures is usually determined as the limit load, i.e., not taking into account the fracture initiation process. In the present work, local approach to fracture was chosen for an analysis of failure initiation, which enabled the behaviour of a structure with a defect to be assessed in accordance with the failure mechanism. An important advantage in comparison with standard fracture mechanics analysis is a possibility to analyze geometries without an initial crack, i.e., to predict the fracture initiation criteria.

The material model used in this paper was the Complete Gurson Model,[14)] which is an extension of the Gurson–Tvergaard–Needleman model.[15–17)] Both models take into account the effects of void nucleation, growth and coalescence on the elastic–plastic behaviour of a material. The advantage of the Complete Gurson Model (CGM) is the lack of necessity for the determination of the critical value of the damage parameter, corresponding to void coalescence and start of sudden loss of load-carrying capacity. In the CGM, this value is calculated during the finite element analysis based on the plastic limit load in the ligament between the voids,[18)] and depends on the stress and strain fields in the structure.

*Corresponding author, E-mail: bmedjo@tmf.bg.ac.rs

Table 1 API J55 steel: chemical composition (mass%).

C	Si	Mn	P	S	Cr	Ni	Mo	V	Cu	Al
0.29	0.23	0.96	0.013	0.022	0.1	0.058	0.012	0.003	0.13	0.025

Table 2 Microstructural parameters.

Material	f_v	λ/μm
API J55 steel	0.027648 (= 2.7648%)	69.39

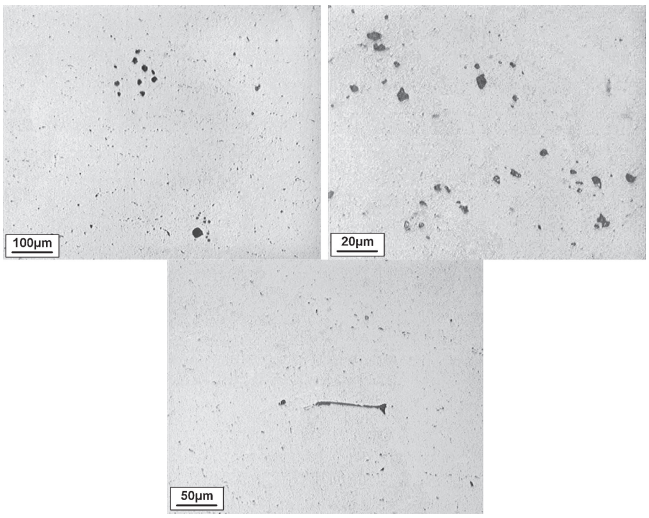

Fig. 1 Micro-photographs of inclusions in the examined material—polished surface.

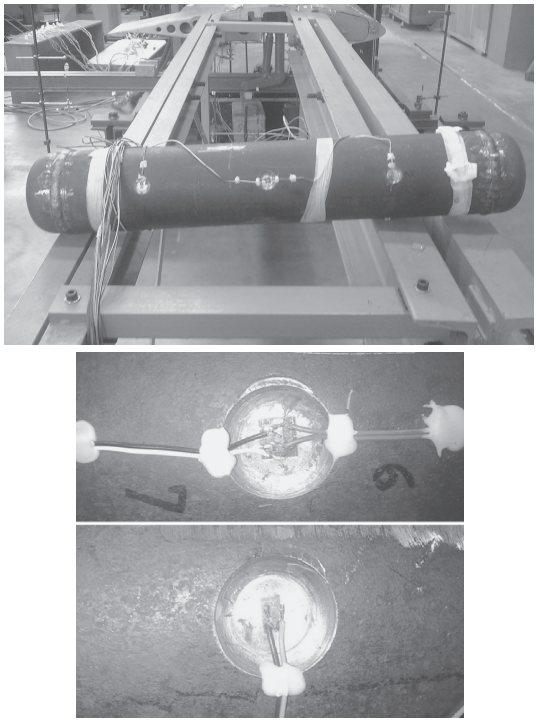

Fig. 2 The pipe prepared for the pressure testing and machined defects with strain gauges.

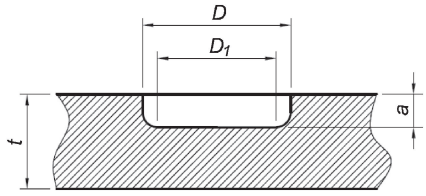

Fig. 3 Dimensions of the defects.

2. Experimental

2.1 Material properties

The chemical composition of the API J55 steel used for the fabrication of the examined seam casing pipe is given in Table 1.[19] The microstructural observation conducted on polished samples cut from the pipe indicated the presence of oxides, silicates and complex oxide inclusions. Three micro-photographs with larger clusters/groups of inclusions are given in Fig. 1. The microstructural parameters (Table 2) were determined by quantitative microstructural analysis. First, the volume fraction of non-metallic inclusions f_v was determined on the cut and polished surfaces. Based on the value of f_v, mean free path between these particles λ is calculated subsequently, in accordance with ASTM 1245 standard.

The tensile properties were determined on round tensile (RT) specimens, also taken from the examined casing pipe. The yield strength was 380 MPa, the ultimate tensile strength was 562 MPa and the hardening exponent was 0.16. All specimens exhibited a ductile fracture mechanism, with necking in the fracture zone. More details on the properties of the material were given previously.[19]

2.2 Pipe pressure testing

Pressure test was conducted on a vessel with simulated circular-shaped defects. The vessel was made from a part of the casing pipe capped at both ends, with nominal dimensions: diameter ϕ 139.7 mm and wall thickness 6.98 mm. Corrosion defects are simulated by machining circular notches at the outer surface of the pipe (Fig. 2). Different levels of material degradation (local thin areas) were represented by varying the depth of these holes a (Fig. 3): 5.25 mm for 75%, 3.5 mm for 50% and 1.75 mm for 25%. Strain gauges were placed at the bottom of each notch, measuring strains in circumferential (hoop) and longitudinal (axial) pipe direction.

3. FEM Calculations

The numerical analysis of the behaviour of the pipe with machined defects under internal pressure was conducted using the finite element (FE) software package Abaqus.[20] The FE meshes consisted of 20-node reduced integration elements, Fig. 4(a). The Gurson yield criterion was used to model the behaviour of the material, including damage development, which will be discussed in the remainder of the text. Due to the symmetry, one quarter of the pipe was modelled, with appropriate boundary conditions defined at the model boundaries. These conditions, i.e., symmetry with respect to the corresponding planes, are schematically shown in Fig. 4(a). Loading is defined by applying a pressure p at the inner surface, with an additional axial loading p_a

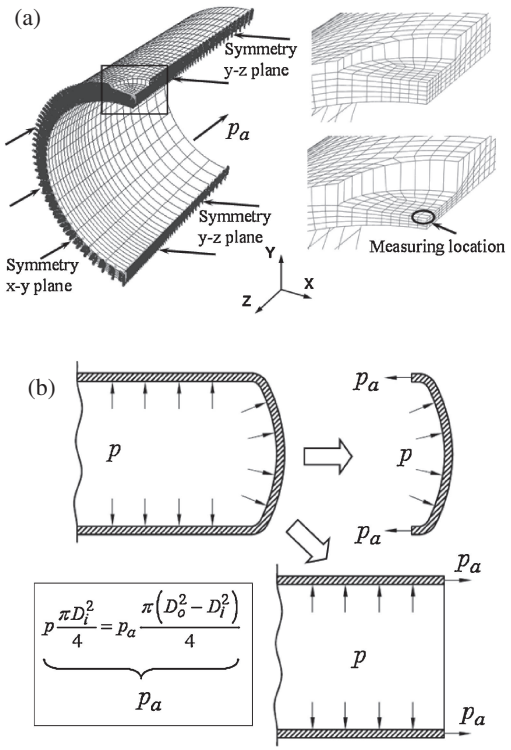

Fig. 4 Finite element meshes with boundary conditions (a) and axial loading p_a, introduced to replace the dished end (b).

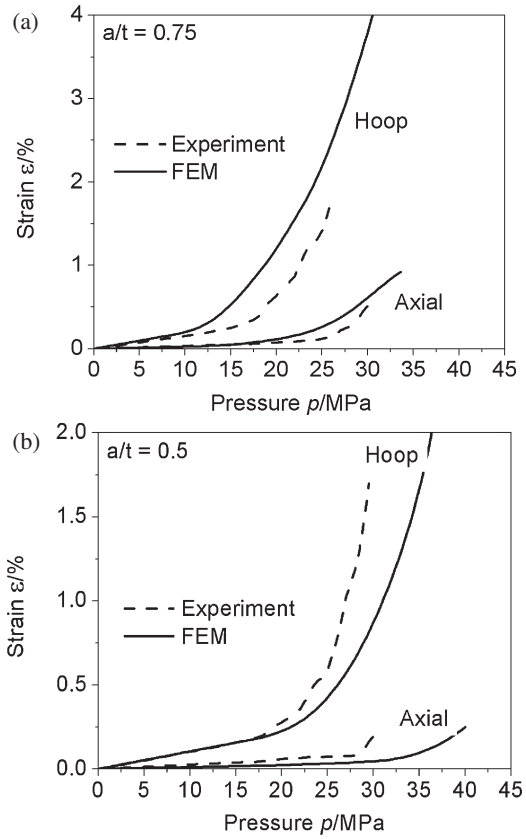

Fig. 5 Comparison of strain values obtained experimentally and numerically, for defects with depth 75% (a) and 50% (b) of the pipe wall thickness.

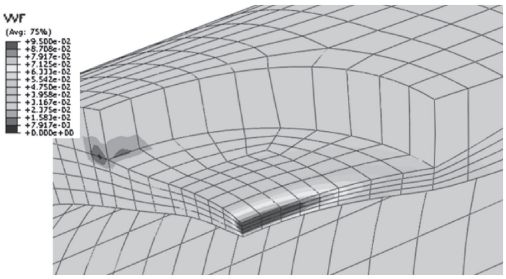

Fig. 6 Distribution of void volume fraction (damage parameter) for the 75% defect, at the moment when local failure criterion is reached.

introduced at one end of the FE model to take into account the fact that the pipe was capped at both ends, Fig. 4(b). Bearing in mind that the strains are measured (in the longitudinal and circumferential direction) in the middle of each defect during the experiment, in the numerical analysis, these values were determined in the FE nearest to that location (marked in Fig. 4(a)).

The results of the numerical analysis predict significantly larger strains in the circumferential direction in comparison with the longitudinal direction (up to 10 times), which was also found from the experiment results, Fig. 5. These results can be explained by the influence of a defect on the stress/strain state, i.e., the more significant relative reduction of the longitudinal cross-section (exposed to hoop stress) in comparison with the cross-section exposed to axial stress. Therefore, the ratio of the hoop stress and the axial stress is significantly larger than in a defect-free geometry (e.g., for a thin-walled cylindrical geometry subjected to internal hydrostatic pressure, the hoop stress is two-times larger than the axial one).

Due to the stress concentration, there is also a significant accumulation of equivalent plastic strain in the bottom of a defect. Damage parameter of the Gurson–Tvergaard–Needleman (GTN) model (porosity or void volume fraction f) also exhibits localization in this area (Fig. 6), which is expected because it depends on the plastic strain, eq. (3).

The expression for the plastic potential in the GTN model[15–17] is:

$$\phi = \left(\frac{\sigma_{\mathrm{eq}}}{\sigma}\right)^2 + 2q_1 f^* \cosh\left(\frac{3q_2\sigma_{\mathrm{m}}}{2\sigma}\right) - [1 + (q_1 f^*)^2] = 0 \tag{1}$$

where σ denotes the flow stress of the material matrix, σ_{m} is the mean stress and σ_{eq} is the von Mises equivalent stress. Constitutive parameters q_1 and q_2 were introduced by Tvergaard[16] to improve the ductile fracture prediction of the Gurson Model (values $q_1 = 1.5$ and $q_2 = 1$ were used here, according to[16]) and f^* is the damage function:[17]

$$f^* = \begin{cases} f & \text{for} \quad f \le f_{\mathrm{c}} \\ f_{\mathrm{c}} + K(f - f_{\mathrm{c}}) & \text{for} \quad f > f_{\mathrm{c}} \end{cases} \tag{2}$$

where f_{c} is the critical value of f, at the moment when the void coalescence begins.

In the initial stage of the ductile fracture of steel, the voids nucleate mainly around non-metallic inclusions. Hence, the initial porosity f_0 is here assumed to be equal to the volume fraction of non-metallic inclusions f_{v}, Table 2. This is equivalent to the assumption that all voids are initiated at a

low loading level, bearing in mind that new (secondary) voids in steel are typically formed during the final stage of fracture, whereas ductile fracture initiation was the subject of this study. Such an approach, i.e., setting the value of f_0 to be equal to the volume fraction of non-metallic inclusions in steel, was applied previously.[21–25] In addition, the volume fraction of larger void-nucleating particles was used as the initial void volume fraction in nodular cast iron[26,27] and aluminium alloys.[28–30]

The growth of the voids during increasing loading is defined by the following expression:

$$\dot{f}_{\text{growth}} = (1-f)\dot{\varepsilon}_{\text{ii}}^{\text{p}} \tag{3}$$

where $\dot{\varepsilon}_{\text{ii}}^{\text{p}}$ is the plastic part of the strain rate tensor.

Zhang *et al.*[14] applied the Thomason void coalescence criterion (based on the plastic limit load[18]) to the GTN model, obtaining the Complete Gurson Model - CGM. The criterion for the beginning of void coalescence is:

$$\frac{\sigma_1}{\sigma} > \left[\alpha\left(\frac{1}{r}-1\right)+\frac{\beta}{\sqrt{r}}\right](1-\pi r^2),$$
$$r = \sqrt[3]{\frac{3f}{4\pi}e^{\varepsilon_1+\varepsilon_2+\varepsilon_3}}\Bigg/\left(\frac{\sqrt{e^{\varepsilon_2+\varepsilon_3}}}{2}\right) \tag{4}$$

where σ_1 is maximum principal stress, ε_1, ε_2, ε_3 are principal strains, r is the void space ratio, α and β are constants fitted by Thomason ($\alpha = 0.1$ and $\beta = 1.2$); Zhang *et al.*[14] proposed a linear dependence of α on the hardening exponent n, which is applied in the CGM.

Unlike the GTN model, the critical void volume fraction f_c does not have to be an input for the CGM, but is a variable that is calculated during the analysis. This value, corresponding to ductile fracture initiation, is taken as the pipe failure criterion in the present study; the CGM was applied through the Abaqus UMAT subroutine created by Zhang, based on Ref. 14). The value of f was monitored in the element nearest to the middle of the defect. When it reached the critical value f_c, pipe failure is predicted and the corresponding pressure was determined.

In the literature,[31–33] the GTN model has been previously used for analysis of the load carrying capacity of pipes with crack-like flaws. The present work aims at extending this approach to pipes containing blunt surface defects, such as those caused by local corrosion. Local approach to fracture was previously applied for similar purposes,[11] but the procedure included so-called uncoupled modelling — calculating the damage parameter during a post-processing procedure, without its influence on the yield criterion.

In addition to circular defects, corresponding to the machined ones, defects with larger lengths were also analysed using FEM, because this defect dimension also affects the maximum pipe pressure. The aim was to establish the relation between these lengths and the load carrying capacity of the pipe. One such defect (the depth is 75% of the pipe wall thickness, $L/\sqrt{Rt} = 5$) is shown in Fig. 7.

The defect area exhibits a reduction in thickness under internal pressure, which corresponds to local necking prior to final failure. This thickness reduction, obtained by FEM, is given in Fig. 8, in which a circular defect is given as an example; both non-deformed and deformed configurations

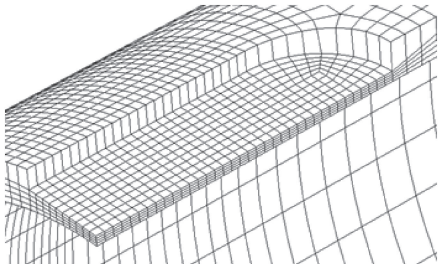

Fig. 7 Finite element mesh of a defect with $L/\sqrt{Rt} = 5$.

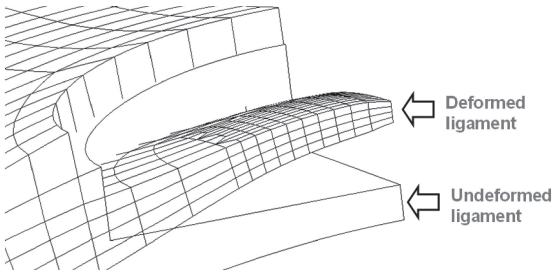

Fig. 8 Ligament - thickness reduction.

are shown. Such material behaviour can be compared to necking of the round tensile specimen, with significant strain localization.

4. Failure Criteria

In addition to the micromechanical criterion, which predicts failure by fracture initiation, several limit load solutions (with plastic collapse as the failure criterion) from the literature were also applied for the calculation of the maximum pressure of the analysed pipe: ASME B31G code, modified ASME B31G and the solution of Choi[6] (in the remainder of the paper – the Choi solution/equation). The corresponding expressions are given in Table 3. In Table 3, a and L are the defect depth and length, M is a geometry correction factor, while C_j ($j = 0.2$) are coefficients in the Choi equation. D_e and D_i represent the external and internal diameter of the pipe, respectively, ($D_i = D_e - 2t$), while the mean pipe radius is $R = (D_e + D_i)/4$.

The dependence of the maximum pressure in a damaged pipeline on the defect length is shown in Fig. 9 for damage levels 75 and 50%; the results were obtained using expressions from Table 3, the FE stress-based solution and the CGM solution. FE stress-based failure criterion is considered to be fulfilled when the von Mises stress value reaches the reference stress throughout the entire ligament, i.e., it is also a plastic collapse criterion, like the three expressions from Table 3. The reference stress was chosen as 85% of the ultimate tensile strength, as a moderately conservative solution.[34]

The Choi procedure gives more conservative results for long and deep defects in comparison to the results of the two ASME methods, while in other cases, it is less conservative. The local approach (the CGM) can predict the trend of decrease in maximum pressure with increasing defect length and depth. Bearing in mind that this approach is strain-based and that it includes damage development in a material, it is

Table 3 Expressions used for calculation of maximum pressure; 1 - ASME B31G, 2 - Modified ASME B31G, 3 - Choi's solution.

1	$L \le \sqrt{20 \cdot D_e t}$	$p_{max} = 1.1 \cdot \sigma_Y \frac{2t}{D_e}\left[\frac{1-\frac{2a}{3t}}{1-\frac{2a}{3t}\cdot\frac{1}{M}}\right]$	$M = \sqrt{1+0.8\frac{L^2}{D_e t}}$
	$L > \sqrt{20 \cdot D_e t}$	$p_{max} = 1.1 \cdot \sigma_Y T \frac{2t}{D_e}\left(1-\frac{a}{t}\right)$	$M = \infty$
2	$L \le \sqrt{50 \cdot D_e t}$	$p_{max} = (1.1 \cdot \sigma_Y + 69 \cdot 10^6)\frac{2t}{D_e}\left(\frac{1-0.85\frac{a}{t}}{1-0.85\frac{a}{t}\cdot\frac{1}{M}}\right)$	$M = \sqrt{1+0.6275\frac{L^2}{D_e \cdot t}-0.003375\left(\frac{L^2}{D_e t}\right)^2}$
	$L > \sqrt{50 \cdot D_e t}$		$M = 3.3+0.032\frac{L^2}{D_e t}$
3	$L < 6\sqrt{Rt}$	$p_{max} = 0.9 \cdot \sigma_m \frac{2t}{D_i}\left[C_2\left(\frac{L}{\sqrt{Rt}}\right)^2 + C_1\left(\frac{L}{\sqrt{Rt}}\right)+C_0\right]$	$C_2 = 0.1163\left(\frac{a}{t}\right)^2 - 0.1053\left(\frac{a}{t}\right)+0.0292$ $C_1 = -0.6913\left(\frac{a}{t}\right)^2 + 0.4548\left(\frac{a}{t}\right)-0.1447$ $C_0 = 0.06\left(\frac{a}{t}\right)^2 - 0.1035\left(\frac{a}{t}\right)+1.0$
	$L \ge 6\sqrt{Rt}$	$p_{max} = \sigma_m \frac{2t}{D_i}\left[C_1\left(\frac{L}{\sqrt{Rt}}\right)+C_0\right]$	$C_1 = 0.0071\left(\frac{a}{t}\right)-0.0126 \quad C_0 = -0.9847\left(\frac{a}{t}\right)+1.1101$

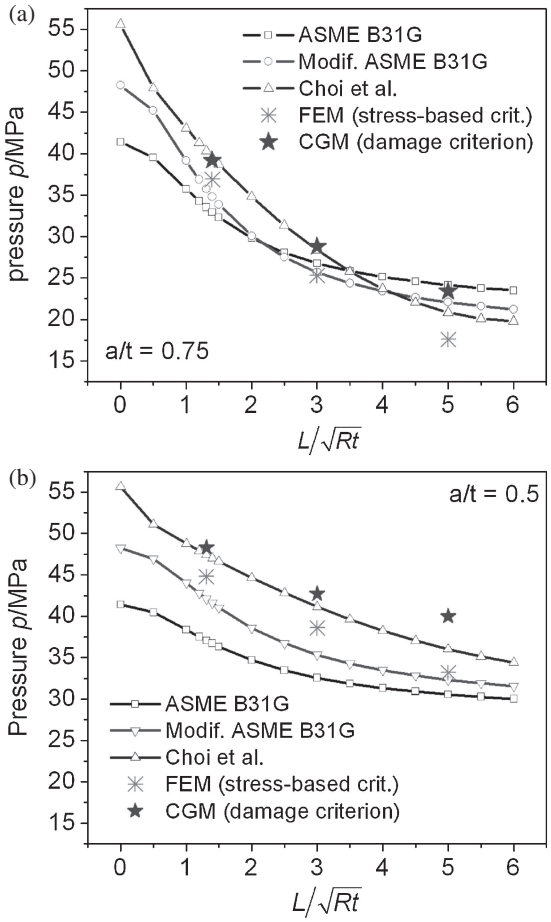

Fig. 9 Maximum pressure for defects with depth 75 and 50% of the pipe wall thickness — dependence on defect length.

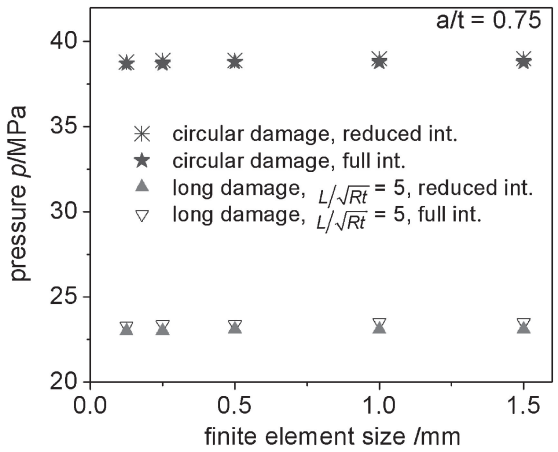

Fig. 10 Maximum pressures for defects with depth 75% — influence of finite element size and integration order.

physically suitable for the materials often used for the manufacture of pipes. Namely, such materials exhibit ductile fracture behaviour under working conditions (except for those operating at very low temperatures, which can also exhibit the brittle fracture mechanism). Local approach also circumvents another problem associated with standard stress-based FE criteria, which is the variable coefficient that is multiplied with the ultimate tensile strength for the determination of the failure criterion.[8] This coefficient, often designated as η, can have values from 0.8 to 1.0, depending on the material (its stress–strain curve, etc.) and geometry of the pipe/defect. As mentioned previously, this value is 0.85 in the Fig. 9. The deviation of the result of the local approach for the model with a depth of 50% of the pipe wall thickness and length $L = 5\sqrt{Rt}$ [right hand side of Fig. 9(b)] may be attributed to the different failure mode, i.e., plastic collapse.

Bearing in mind that the prediction of the initiation of ductile fracture using the local approach to fracture typically exhibits mesh dependency, the calculations were performed with mesh refinement in the radial, axial and thickness direction, in order to check the effect of element size and formulation on the load carrying capacity. All the changes were made in the defect ligament because high stress and strain values are localized in this area. It could be concluded that the results did not vary significantly (Fig. 10; element

size denotes the size of its longest side, in the plane of the defect), which can be attributed to the fact that crack initiation is assessed in this work as a failure criterion, and the stress concentration on the analysed geometries was not pronounced. The modelling of a structure with a crack (once the crack has been initiated) using a micromechanical model would require the determination of the specific element size for the crack region and ligament in front of the crack tip.[35,36] This element size (or distance between the integration points) is typically related to the mean free path λ between non-metallic inclusions. However, in this case the element size and formulation have very small effect, bearing in mind that crack initiation was analysed on geometry without a pre-crack.

5. Conclusions

This paper deals with the criteria for the assessment of the residual strength of damaged pipes, and the conclusions can be summarised as follows:

Unlike other numerical procedures for the assessment of pipe integrity, mainly stress based, micromechanical modelling includes analysis of damage initiation that inevitably emerges prior to failure. This approach enables the user to analyse fracture initiation in structures without a pre-crack (i.e., with notches, local thin areas, etc.), which can not be achieved by application of fracture mechanics criteria.

Observing the stress state in the middle of a defect revealed that the maximum pressure obtained using the local approach gives similar values for API J55 steel as the stress-based criterion (requiring that von Mises equivalent stress reaches the reference stress throughout the entire ligament). However, an advantage of the local approach is the lack of a necessity for an estimation of the reference stress - in the literature varying between 80 and 100% of the ultimate tensile strength.

An influence of the FE mesh on the applied micromechanical criterion for pipe failure exists, but it is not significant. The mesh dependence is much more pronounced if this criterion is applied to pre-cracked structures.

Acknowledgements

The authors acknowledge the support from the Serbian Ministry of Science under the projects ON 174004 and TR 35002. BM, MR and MZ acknowledge the partial support from the Serbian Ministry of Science under the project E!5348. The authors would also like to thank Z. L. Zhang for the CGM user subroutine and I. Cvijović-Alagić for help in microstructural analysis.

REFERENCES

1) American Society of Mechanical Engineers: ASME B31G - Manual for determining the remaining strength of corroded pipelines, New York, (1991).
2) J. Kiefner and P. Vieth: A modified criterion for evaluating the strength of corroded pipe-Final Report on project PR 3-805, (the Pipeline Supervisory Committee of the American Gas Association, Ohio: Battelle, 1989).
3) J. Kiefner and P. Vieth: Oil Gas J. **88** (1990) 56–59.
4) D. Norske Veritas: DNV RP-F101, Corroded pipelines-recommended practice, Hovik, (2004).
5) http://www.eurofitnet.org
6) J. B. Choi, B. K. Goo, J. C. Kim, Y. J. Kima and W. S. Kim: Int. J. Press. Vessels Piping **80** (2003) 121–128.
7) H. Adib-Ramezani, J. Jeong and G. Pluvinage: Int. J. Press. Vessels Piping **83** (2006) 420–432.
8) M. Chiodo and C. Ruggieri: Int. J. Press. Vessels Piping **86** (2009) 164–176.
9) SINTAP: Structural integrity assessment procedure, Final report EU project BE95-1462, Brussels, (1999).
10) A. Cosham, P. Hopkins and K. A. Macdonald: Eng. Fail. Anal. **14** (2007) 1245–1265.
11) C. K. Oh, Y. J. Kim, J. H. Baek, Y. P. Kim and W. S. Kim: Int. J. Press. Vessels Piping **84** (2007) 512–525.
12) B. N. Leis and X. K. Zhu: Corrosion assessment criteria, Report, (U.S. Department of Transportation, Batelle, Columbus, 2005).
13) G. Wilkowski, D. Stephens, P. Krishnaswamy, B. Leis and D. Rudland: Nucl. Eng. Des. **195** (2000) 149–169.
14) Z. L. Zhang, C. Thaulow and J. Odegard: Eng. Fract. Mech. **67** (2000) 155–168.
15) A. L. Gurson: J. Eng. Mater. Tech. - T. ASME **99** (1977) 2–15.
16) V. Tvergaard: Int. J. Fract. **17** (1981) 389–407.
17) V. Tvergaard and A. Needleman: Acta Metall. **32** (1984) 157–169.
18) P. F. Thomason: *Ductile Fracture of Metals*, (Pergamon Press, Oxford, 1990).
19) Ž. Šarkoćević, M. Arsić, B. Medjo, D. Kozak, M. Rakin, Z. Burzić and A. Sedmak: Strojarstvo: J. Theory Appl. Mech. Eng. **51** (2009) 303–311.
20) Abaqus FEM software package,www.simulia.com
21) J. Besson, D. Steglich and W. Brocks: Int. J. Plast. **19** (2003) 1517–1541.
22) A. Nonn, W. Dahl and W. Bleck: Eng. Fract. Mech. **75** (2008) 3251–3263.
23) N. Benseddiq and A. Imad: Int. J. Press. Vessels Piping **85** (2008) 219–227.
24) I. Penuelas, C. Betegon and C. Rodriguez: Eng. Fract. Mech. **73** (2006) 2756–2773.
25) V. Uthaisangsuk, U. Prahl, S. Muenstermann and W. Bleck: Comput. Mater. Sci. **43** (2008) 43–50.
26) D. Steglich and W. Brocks: Fatigue Fract. Eng. Mater. Struct. **21** (1998) 1175–1188.
27) M. J. Dong, C. Prioul and D. Francois: Metall. Mater. Trans. A **28A** (1997) 2255–2262.
28) T. Pardoen, F. Scheyvaerts, A. Simar, C. Tekoglu and P. Onck: C. R. Phys. **11** (2010) 326–345.
29) P. Cambresy: GKSS report 2006/5, (GKSS-Forschungszentrum, Geesthacht, 2006).
30) W. Brocks, K.-H. Schwalbe and U. Zerbst: Adv. Eng. Mater. **8** (2006) 319–327.
31) B. Bezensek and K. Miyazaki: Proc. 2009 ASME Pressure Vessels and Piping Division Conference, Prague, Czech Republic, (2009) published on CD.
32) F. Dotta and C. Ruggieri: Int. J. Press. Vessels Piping **81** (2004) 761–770.
33) S. Saxena, N. Ramakrishnan and J. S. Chouhan: Eng. Fract. Mech. **77** (2010) 1058–1072.
34) M. Arsić, M. Rakin, Ž. Šarkoćević, B. Medjo, Z. Burzić and A. Sedmak: Int. J. Press. Vessels Piping (2011) submitted.
35) M. Rakin, Z. Cvijovic, V. Grabulov, S. Putic and A. Sedmak: Eng. Fract. Mech. **71** (2004) 813–827.
36) B. Medjo, M. Rakin, N. Gubeljak, M. Arsić and A. Sedmak: Proc. 18th European Conference on Fracture, Dresden, Germany, (2010) published on CD.